



## OPEN Studying the impacts of land use types and soil textures on agricultural drought in Ziya river basin using SWDI

Yuefen Zhang<sup>1,3</sup>, Yimin Hao<sup>2✉</sup>, Jiyang Tian<sup>1,3</sup>, Qingqing Zhang<sup>4✉</sup>, Ronghua Liu<sup>1,3</sup> & Jianzhu Li<sup>2</sup>

Agricultural drought (AD) refers to a decline in crop yield as a result of a decrease in soil moisture, which is closely associated with land use type and soil texture. In semi-arid climates, however, it is unclear what role land use type and soil texture play in AD. Here, soil water deficit index (SWDI) considering the physiological state of vegetation is used to characterize AD. This study systematically investigated the effects of land use type and soil texture on the evolution of AD, and also analyzed the temporal changes of soil moisture, water deficiency in the vadose zone, and precipitation at annual and monthly scales. The results indicate that there is a broad similarity between the annual variation trends of soil moisture and precipitation in the Ziya River Basin (ZRB), while water shortages in the vadose zone are opposite. It is evident that SWDI has good applicability in characterizing AD in ZRB by comparing it with meteorological drought (MD). For impacts of different land use types and soil textures, Forest and Grassland exhibit greater drought resistance with the lowest duration ( $D$ , 4.12 and 3.92) and severity ( $S$ , 7.76 and 7.93), whereas Cropland, Waters, and Urban Land ( $D > 5.39$ ;  $S > 11$ ) are more susceptible to severe droughts. For soil textures, Sand ( $D$ , 4.56;  $S$ , 8.32) and Loam ( $D$ , 5.09;  $S$ , 10.32) are more prone to AD than Clay ( $D$ , 3.24;  $S$ , 5.13). Overall, these findings contribute to understanding the role of the land use types and soil textures in the evolution of AD in semi-arid regions and provide practical recommendations for early identifying AD.

**Keywords** Agricultural drought, Soil water deficit index, Land use types, Soil texture

Agricultural drought (AD) is a recurring, long-lasting and unstructured natural disaster in all lands of the world<sup>1–3</sup>, which is the result of many factors, such as hydrological conditions, meteorological conditions, crop layouts, crop varieties and growth conditions, farming system and tillage level<sup>4</sup>. Since the beginning of the 21st century, the average annual grain loss due to drought in China is 37.284 million tons, about twice the grain loss in the 1980s, accounting for 7.7% of the total grain production in the same period<sup>5</sup>. Therefore, understanding and evaluating AD is of great significance to improve the ability of drought resistance and disaster reduction, ensure food security, and promote the sustainable development of social economy and environment<sup>6–10</sup>.

Soil moisture is widely considered to be an important indicator for monitoring AD, as water stress on crops is closely related to soil moisture content<sup>11–14</sup>. The essence of AD is that soil water shortage cannot meet the water demand of vegetation roots<sup>15,16</sup>. The traditional AD monitoring method mainly comes from the station data<sup>17,18</sup>, which is difficult to realize the macro dynamic monitoring of AD due to its low efficiency and lack of representativeness<sup>10,18</sup>. Compared with traditional AD monitoring methods, remote sensing monitoring methods can realize large-area and dynamic monitoring by using the spectral, spatial and azimuth information of surface objects, and can also dynamically monitor soil moisture content<sup>19–21</sup>. While recent reanalysis and remote sensing soil moisture data are typically available at coarse resolution and remote sensing data are limited

<sup>1</sup>State Key Laboratory of Water Cycle and Water Security, Institute of Water Resources and Hydropower Research, Beijing 100038, China. <sup>2</sup>State Key Laboratory of Hydraulic Engineering Intelligent Construction and Operation, Tianjin University, Tianjin 300350, China. <sup>3</sup>Research Center on Flood & Drought Disaster Reduction, Ministry of Water Resources, Beijing 100038, China. <sup>4</sup>Key Laboratory of Water Ecology Remediation and Protection at Headwater Regions of Big Rivers, Ministry of Water Resources, Xining 810016, China. ✉email: 934060679@qq.com; 1256737600@qq.com

to surface soil<sup>19,22–26</sup>, high-quality gridded soil moisture products are essential for many Earth system science applications<sup>27–30</sup>.

AD monitoring indices based on soil moisture can be classified into two categories: The first type of index requires long-term soil moisture data to determine the extent to which the current soil moisture deviates from the historical normal range, such as standardized soil moisture index (SSMI), soil moisture anomaly index (SMAI), soil moisture percentile (SMP). Such indicators only need soil moisture data, and the monitoring results in different regions are comparable. The disadvantage is that the time series is required to be long enough. The second category realizes AD monitoring based on soil moisture and soil hydraulics parameters, such as soil moisture index (SMI) and soil water deficit index (SWDI)<sup>31</sup>. The advantage of this type of index is that from the perspective of soil available water, the influence of soil properties in different regions on water deficit is considered. However, for regional AD monitoring, it is difficult to accurately obtain soil attribute parameters in different regions. From the perspective of AD monitoring, SWDI considers the relationship between a plant physiological state and soil water and is more suitable for monitoring AD. Previous studies have shown that SWDI can well reflect the relationship between soil moisture and AD at both basin scale and regional scale and is considered as a potential indicator for AD monitoring<sup>32–36</sup>.

The spatial distribution of soil moisture varies greatly due to the diversity of soil types, land use/land cover, topography and soil textures. With the deepening influence of climate change and human activities, drought appears to be widespread and frequent. Land use/cover change, as a man-made “system disturbance”, is one of the main driving factors affecting the spatio-temporal evolution of drought events in river basins<sup>37,38</sup>. In addition, soil texture is closely related to soil water content. The water capacity of different soil textures in farmland is different, and the effective water content of soil and plants is also different. However, how different soil textures affect the evolution of AD is closely related to the response of soil water to AD under different soil textures<sup>39</sup>. Therefore, it is necessary to systematically study the effects of land use types and soil textures on the evolution of AD in semi-arid areas.

The purpose of this study is to evaluate the impacts of land use types and soil textures on AD in ZRB, by using the widely used and effective SWDI. Specifically, the objectives of this study are: (1) to investigate the feasibility of SWDI in a semi-arid area; (2) to evaluate the impacts of different land use types on AD; and (3) to evaluate the impacts of different soil textures on AD.

In the following, Sect. “Materials and methods” describes the materials and methods. The impacts of different land use types and soil textures on AD are presented in Sect. “Study area”, with a specific focus on comparing average SWDI time series and violin graphs of drought characteristics of AD. Discussion is presented in Sect. “Data”, followed by the conclusions summarized in Sect. “Methodology”.

## Materials and methods

### Study area

As a subbasin of the Haihe River Basin, the Ziya River Basin (ZRB, 36° 3' N to 39° 5' N, 112° 20' E to 116° 0' E) is situated in a semi-arid and warm temperate continental monsoon climate zone and covers 46,328 km<sup>2</sup>. The upper reaches of the basin are located at the eastern foot of the Mountains, where the terrain uplift is relatively obvious, precipitation is relatively abundant, and the temperature is relatively low, showing certain characteristics of mountain climate. The terrain in the middle and lower reaches of the plain is flat, with slightly less precipitation, higher temperatures, more vigorous evaporation and more prominent continental climate characteristics (Fig. 1).

In recent years, it has been observed that land use types have not changed significantly over ZRB<sup>40</sup>. For purposes of this study, the land use types in 2010 were chosen in order to better match the data period (2000–

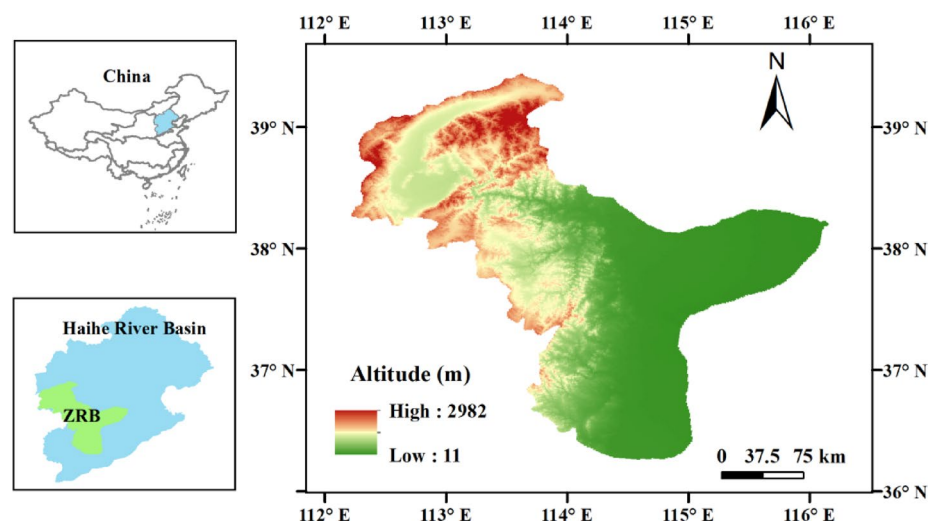


**Fig. 1.** Map showing the location of Ziya River Basin (ZRB). The figure is created in ArcMap 10.3 (<https://desktop.arcgis.com/zh-cn/desktop/index.html>).

2018, see Sect. “Data”. Data). Figure 2 shows the spatial distribution of (a) land use and (b) soil textures in ZRB. From Fig. 2a, vegetation covers approximately 90% of the basin area (49.86% of Cropland, 15.78% of Forest and 24.38% of Grassland) and there is a very limited amount of Unused land and Waters. Among the soil types (Fig. 2b), Loam accounts for a large proportion (75.98%), Sand represents a small percentage (21.76%), and Clay is the smallest (2.26%).

## Data

Digital elevation model (DEM), land use, soil texture, precipitation, and soil moisture data are the main data sources in this paper. We used the high spatial-resolution (1 km) precipitation data from a long-term (1901–2021) dataset produced by Peng et al. (2020), which is generated in China by Delta spatial downscaling scheme based on global 0.5° climate data set published by Climatic Research Unit and global high-resolution climate data set published by WorldClim database (website address: <https://worldclim.org/>). DEM with a resolution of 30 m was downloaded from the Geospatial Data Cloud website (<http://www.gscloud.cn/search>); the land use data in 2010 come from <http://www.resdc.cn>; Chinese soil data set-based Harmonized World Soil Database (version 1.2) and the monthly rainfall data with a resolution of 1 km from 1961 to 2018 come from <http://www.tpd.ac.cn/zh-hans/>; the SMC11.0 (Soil Moisture of China by in situ data, version 1.0) with a resolution of 1 km from 2000 to 2020 was downloaded from <https://doi.org/10.11888/Terre.tpd.272415>. In order to match the research period of all data, 2000–2018 is selected as the study period in this paper.

## Methodology

### Soil water deficit index

Soil water deficit index (SWDI) is an effective indicator of agriculture drought that quantifies soil moisture deficits associated with drought conditions. According to the Eq. 1, SWDI can be calculated by combining land surface soil moisture and soil water parameters as follows:

$$SWDI = \left( \frac{\theta - 0.8 \times \theta_{FC}}{\theta_{AWC}} \right) \times 10 \quad (1)$$

where  $\theta$  determines the land surface soil moisture ( $\text{m}^3/\text{m}^3$ );  $\theta_{FC}$  and  $\theta_{AWC}$  represent the soil moisture ( $\text{m}^3/\text{m}^3$ ) at field capacity (FC) and at available water capacity (AWC), respectively;  $\theta_{AWC}$  is calculated by subtracting  $\theta_{FC}$  from soil moisture at the wilting point ( $\theta_{WP}$ ), as shown in Eq. 2:

$$\theta_{AWC} = \theta_{FC} - \theta_{WP} \quad (2)$$

The reduction factor is set as 0.8 in this study, indicating that drought occurs when  $\theta$  is less than 0.8 times  $\theta_{FC}$ . Referring to the findings of the following relevant studies, Pan et al. (2014) studied the effect of drought on six plant species on the Tibetan Plateau, they determined the normal level of soil moisture to be more than 0.8 times. According to Wu (2013), the photosynthetic physiological response of three tree species peaks at 0.8 times  $\theta_{FC}$  and declines when soil moisture decreases. A final step is to multiply the index by 10 in order to make the value agronomically relevant in terms of soil water availability.

In the presence of a positive SWDI, the soil moisture is greater than 0.8 times  $\theta_{FC}$ , indicating that there is no AD. Thus, a threshold of 0 is considered to be the point at which drought conditions begin and end. The SWDI was calculated at a monthly time scale, and an overview of the drought classification was provided in Table 1<sup>40,41,42</sup>.

Note: Here SPI, SWDI represent standardized precipitation index and soil water deficit index.

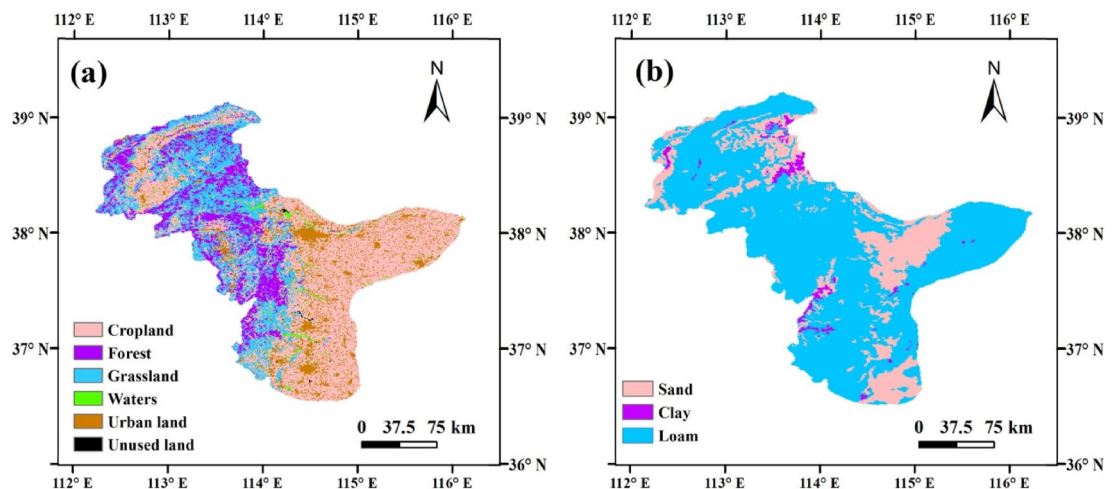


**Fig. 2.** Spatial distributions of (a) land use and (b) soil texture and the corresponding site locations in Ziya River Basin. The figure is created in ArcMap 10.3 (<https://desktop.arcgis.com/zh-cn/desktop/index.html>).

Drought class	SPI	SWDI
No drought	> 0	> 0
Mild drought	-1.0 ~ 0	-2 ~ 0
Moderate drought	-1.5 ~ -1.0	-5 ~ -2
Severe drought	-2.0 ~ -1.5	-10 ~ -5
Extreme drought	≤ -2.0	≤ -10

**Table 1.** Drought categories in accordance with the values of SPI and SWDI.

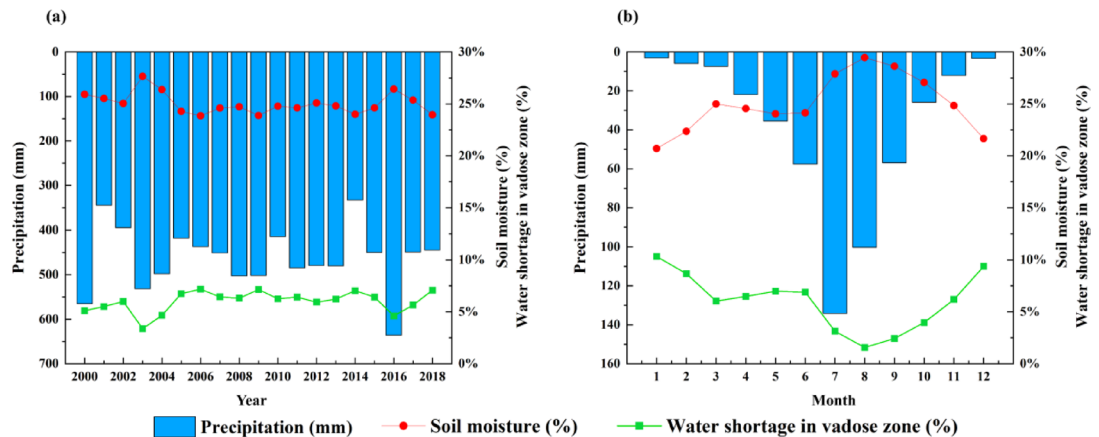


**Fig. 3.** Temporal variations of precipitation, soil moisture and water shortage in vadose zone at (a) annual and (b) monthly scales of Ziya River Basin.

### Standardized precipitation index

SPI is a commonly used metric for assessing meteorological drought (MD)<sup>43–46</sup> on a range of timescales, proposed by McKee et al. (1993). In this study, the SPI and SWDI are compared to analyze the relationships among MD and AD. The gamma probability density function was used to fit precipitation data as follows<sup>47–49</sup>:

$$g(x) = \frac{1}{\beta^\alpha \cdot \Gamma(\alpha)} x^{\alpha-1} \cdot e^{-\frac{x}{\beta}}, \quad x > 0$$

where  $\alpha$  and  $\beta$  ( $> 0$ ) are the shape and scale parameters, respectively; and  $x$  ( $> 0$ ) is the amount of monthly precipitation.

### Water shortage in vadose zone

The vadose zone is the area where atmospheric water and surface water are connected with groundwater and exchange water. It is a complex system of rock and soil particles, water and air. The vadose zone has the ability to absorb water, retain water and transfer water. For ease of calculation, the water shortage of the vadose zone is defined as follows:

$$V = \theta_{FC} - \theta_i \quad (3)$$

where  $V$  is the water shortage of the vadose zone of a certain soil moisture grid, %;  $\theta_i$  is the initial soil moisture content, %.

### Drought characteristics

Drought characteristics, including duration ( $D$ ), and severity ( $S$ ) were extracted by using the Runs theory<sup>50</sup>.  $D$  is the number of consecutive months with both  $SPI < -0.5$ <sup>46,51</sup> and  $SWDI < 0$ <sup>52</sup>;  $S$  is the summation of the absolute values of drought indices for a drought event. To analyze the regional impact of drought, we also use the ratio of drought areas (RDA), which is the percentage of grids where drought occurs compared to the total number of grids in the region. The higher the RDA, the wider the area affected by the drought.

## Results

### Temporal variations of precipitation and soil moisture

In ZRB, annual average soil moisture and annual precipitation show similar trends, with soil moisture increasing as precipitation increases (Fig. 3a). In contrast, the water shortage in the vadose zone decreases with an increase in precipitation. There is an average annual precipitation of 463.95 mm in the watershed; however, in 2001, 2002,

and 2014 the annual precipitation was less than 400 mm, and the minimum value of 332.85 mm appeared in 2014. Statistically, the soil moisture of the watershed is 25.03% on average, while 2006, 2009, 2014 and 2018 are among the years with reduced soil moisture. In the vadose zone of the basin, the average annual water shortage is 6.0%; 2014 is the year that has the highest value of water shortage, which is 7.04%. By analyzing the above information, it is evident that the ZRB is in a situation where soil moisture is scarce in 2014.

Similarly, the interannual distribution of soil moisture and precipitation in the basin is well-consistent, as monthly soil moisture increases with increased precipitation (Fig. 3b). However, as depicted in Fig. 3b, precipitation has increased from January to July, but soil moisture decreased slightly from March to June, and it did not increase until July, indicating that soil moisture has a lag during spring (March to June). There is an uneven distribution of precipitation throughout the year in ZRB, with low precipitation recorded in both October–December and January–April of the following year, and the lowest precipitation recorded in January, only 3.04 mm. In winter, soil moisture is less than 23%, and the minimum value is 20.69% in January, which coincides with the month of the minimum precipitation. It is noticeable that the vadose zone exhibits a water shortage of more than 8% between January and February as well as December of each year, with the maximum showing up in January at 10.33%, followed by a shortage of 8.68% and 9.38% in December and February. Overall, winter is the most prominent season when soil moisture levels are low in ZRB.

### Investigation into the feasibility of SWDI in the study area

The Run theory is used to identify drought events of MD and AD, and the accuracy of SWDI at the monthly scale is verified by comparing the drought characteristics of the two. Table 2 represents the drought characteristics sequences for MD and AD in ZRB from 2000 to 2018, and the most significant drought events with a long duration and high severity are indicated in red color. As shown in Table 2, it is believed that the time at which AD began and ended is almost in accordance with the time at which MD began and ended, based on the dates from the two sources. The following four typical drought events are taken as examples. In 2005–2006, MD lasted for 20 months with  $S$  of 6.54, while AD had a shorter  $D$  of 11 months with a higher  $S$  of 8.3. In 2008–2009 and 2010–2011, AD and MD are both beginning and ending at the same time, however, AD exhibits a more severe  $S$  (3.35–4.15) than MD (9.08–10.19). Additionally, there have been three small drought events for MD in 2013–2015 resulting in the longest and most severe drought event for AD over the entire study period.

Figure 4 illustrates the temporal variations of RDA under different levels (mild, moderate and severe drought) of AD in ZRB. The extraordinary droughts of 2005–2006, 2008–2009, 2010–2011 and 2013–2015 affected a larger geographic area ( $RDA > 60\%$ ) and had more serious consequences, which is consistent with the findings of Table 2. During 2000–2018, AD was mainly associated with mild droughts, and the number of moderate drought events has increased significantly since 2004, indicating that AD has gradually evolved from mild to moderate in recent years although some mitigation of droughts in 2016–2017. Hence, these analyses suggest that the SWDI calculated in the ZRB is reliable and accurately reflects the soil water balance. It should be noted that AD has become increasingly serious in ZRB in recent years, and more early warnings of drought are required.

No.	MD			AD		
	Beginning-End	D (month)	S	Beginning-End	D (month)	S
1	2001.5-2001.10.5.10.5.10	6	4.34	2000.4-2000.6.4.6	3	3.17
2	2002.1-2002.4.1.4	4	3.05	2001.5-2001.10.5.10.5.10	6	2.59
3	2002.7-2002.8.7.8	2	2.04	2002.3-2002.4.3.4	2	1.65
4	2003.6-2003.8.6.8	3	1.02	2002.8-2002.11.8.11.8.11	4	2.80
5	2004.9-2004.11.9.11.9.11	3	1.86	2004.10-2004.11.10.11	2	0.38
6	<b>2005.3-2006.10.3.10</b>	<b>20</b>	<b>6.54</b>	<b>2005.6-2006.4.6.4</b>	<b>11</b>	<b>8.30</b>
7	2007.7-2007.8.7.8	2	1.16	2006.9-2007.2.9.2	6	5.19
8	<b>2008.7-2009.7.7.7</b>	<b>13</b>	<b>3.35</b>	2007.5-2007.9.5.9	5	4.63
9	2009.12-2010.1.12.1	2	0.68	2008.1-2008.3.1.3	3	1.27
10	2010.4-2010.7.4.7	4	3.36	<b>2008.8-2009.7.8.7</b>	<b>12</b>	<b>10.19</b>
11	<b>2010.10-2011.8.10.8</b>	<b>11</b>	<b>4.15</b>	2009.10-2009.12.10.12	3	1.88
12	2013.3-2013.5.3.5	3	1.55	2010.5-2010.7.5.7	3	2.96
13	<b>2013.10-2014.1.10.1</b>	<b>4</b>	<b>2.98</b>	<b>2010.10-2011.8.10.8</b>	<b>11</b>	<b>9.08</b>
14	<b>2014.5-2014.11.5.11.5.11</b>	<b>7</b>	<b>3.48</b>	2012.5-2012.6.5.6	2	1.15
15	<b>2015.6-2015.8.6.8</b>	<b>3</b>	<b>2.51</b>	2012.10-2013.5.10.5	8	3.50
16	2016.3-2016.5.3.5	3	1.40	<b>2013.8-2015.8.8.8</b>	<b>25</b>	<b>17.52</b>
17	2016.8-2016.9.8.9	2	0.82	2016.4-2016.5.4.5	2	1.12
18	2017.6-2018.3.6.3	10	3.27	2017.5-2017.7.5.7	3	1.85
19	2018.9-2018.11.9.11.9.11	3	3.63	2017.12-2018.3.12.3	4	1.58
20	-	-	-	2018.6-2018.12.6.12.6.12	7	6.84

**Table 2.** The drought characteristics sequences of MD and AD in Ziya river basin during 2000–2018. Note: Here MD, AD,  $D$ ,  $S$  represent meteorological drought, agricultural drought, duration, and severity.

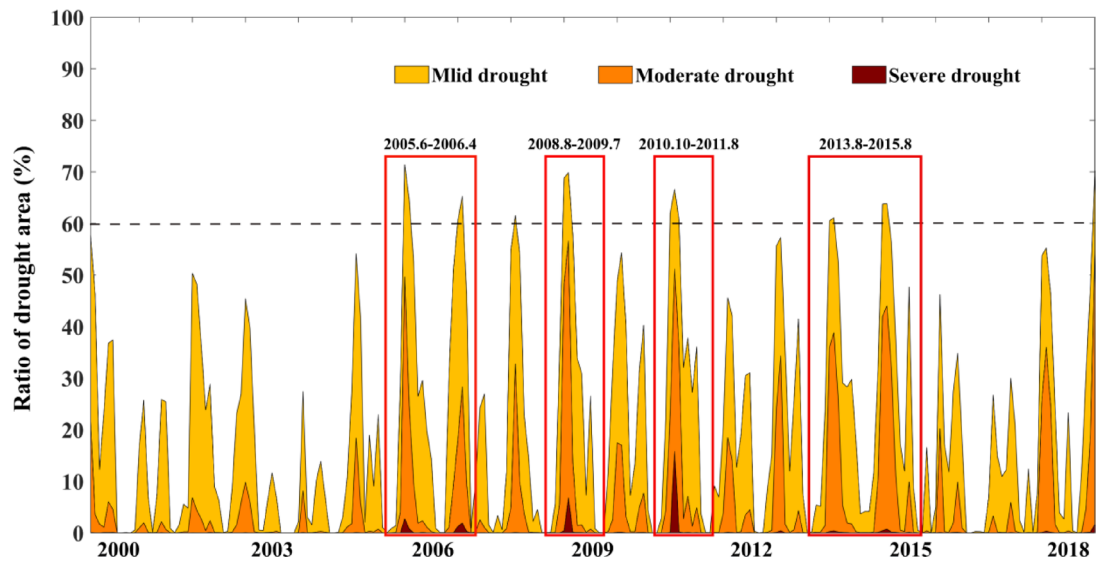


**Fig. 4.** Temporal variations of ratio of drought areas under different levels of agricultural drought in Ziya River Basin.

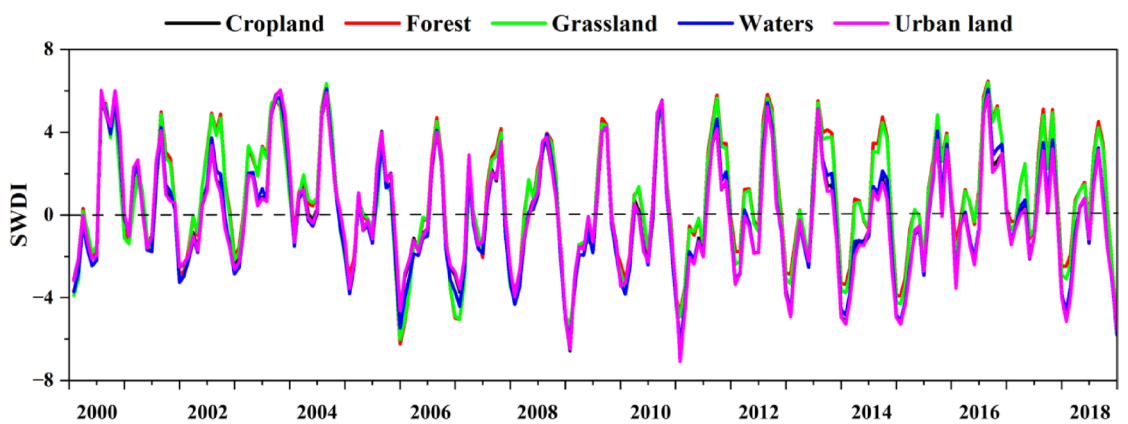
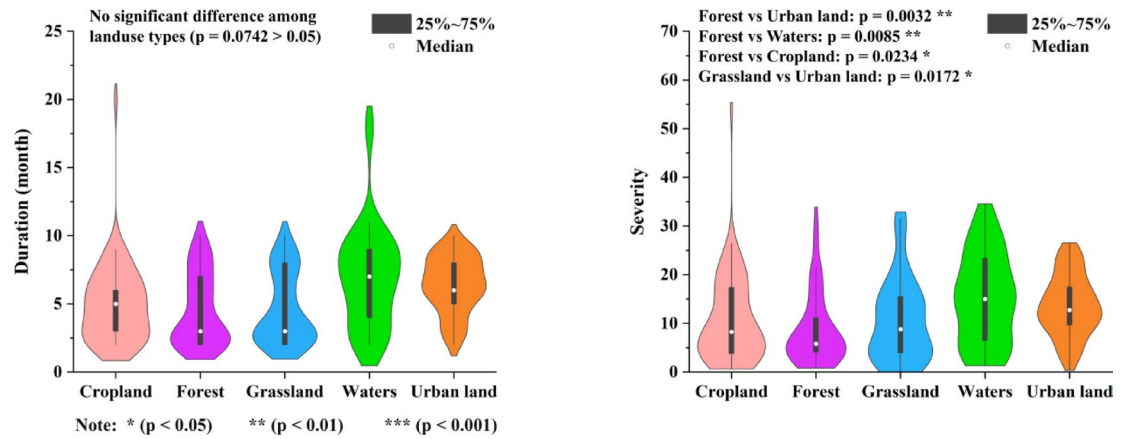


**Fig. 5.** Average soil water deficit index (SWDI) timeseries during 2000–2018 for each type of land use in Ziya River Basin.

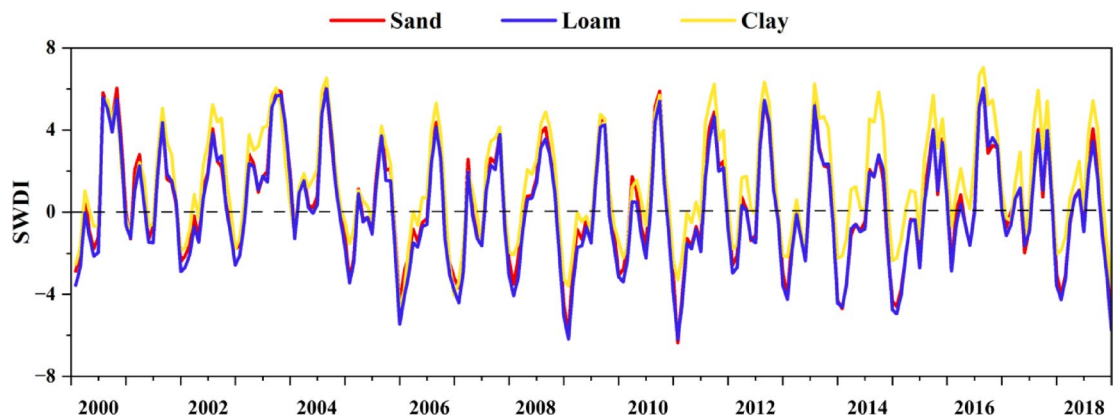
### Impacts of land use types on AD

Figure 5 shows the average SWDI time series during 2000–2018 for each land use type (Cropland, Forest, Grassland, Waters and Urban land, respectively) in ZRB. Generally, there is a similar tendency of AD across different land use types during 2000–2018 (Fig. 5). Also, severe drought events occurred more frequently for all land use types in 2004–2015 with lower SWDI values (more negative), which is consistent with the findings of Fig. 4. As a general rule, more severe droughts can be observed in Cropland, Waters and Urban land than other land use types throughout the entire period. In contrast, it appears that Forest and Grassland are more susceptible to wet events and light droughts with high SWDI, as demonstrated by the years 2002–2003, 2011–2012, 2014 and 2017, although they may suffer from severe droughts in certain cases (such as in 2006). This is possibly due to the fact that Forest and Grassland have higher drought resistance and toughness.

For further investigation of the differences in drought characteristics ( $D$  and  $S$ ) across different land use types (Fig. 6), violin graphs were conducted during 2000–2018 over ZRB. The quantiles range from 25% to 75%, and the white circles represent the mean values. Generally, the mean values of  $D$  (5.81) and  $S$  (11.72) identified by Urban land are highest than other land use types, followed by Cropland ( $D$ , 5.41;  $S$ , 11) and Waters ( $D$ , 5.39;  $S$ , 11.57). Forest and Grassland show the lowest  $D$  (4.12 and 3.92, respectively) and  $S$  (7.76 and 7.93, respectively) over ZRB, leading to the conclusion that Forest and Grassland exhibit more light droughts with shorter  $D$  and lower  $S$  due to their superior water holding capacity. Conversely, Cropland, Waters, and Urban land are prone to severe droughts, which may be caused by increased evaporation and human activity.



**Fig. 6.** Violin graphs of duration and severity of agricultural drought for different land use: Cropland, Forest, Grassland, Waters and Urban land, respectively.



**Fig. 7.** Average soil water deficit index (SWDI) timeseries during 2000–2018 for each type of soil texture in Ziya River Basin.

### Impacts of soil textures on AD

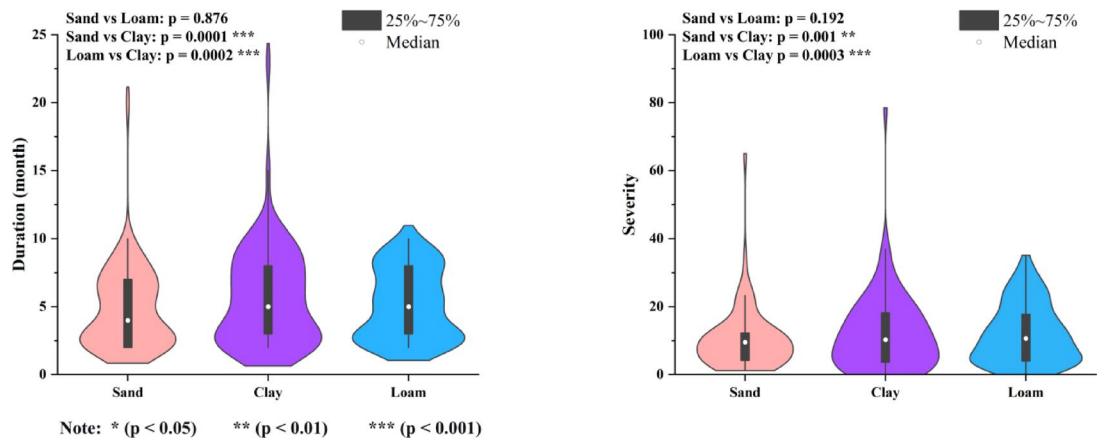
Figure 7 shows the average SWDI time series of AD during 2000–2018 for each type (Sand, Clay, and Loam, respectively) of soil textures in ZRB. Generally, it has been noted that all types of soil textures experienced similar changes in AD during the entire period (Fig. 7). Similarly, it can be found that severe drought events were more frequent for all types of soil textures between 2004 and 2015, and SWDI values were lower (more negative) in most cases. Clay is more likely to experience wet events as well as light droughts with a larger SWDI, whereas the most severe droughts have occurred in Sand and Loam (e.g., 2009, 2011, 2013, 2015, and 2018), indicating that AD occurs more frequently in Sand and Loam.

Figure 8 shows the violin graphs of  $D$  and  $S$  for different soil textures: Sand, Clay, and Loam, respectively, with quantiles ranging from 25% to 75%, and white circles indicating the mean values. Among the three soil textures, Loam has the largest  $D$  (5.09) and  $S$  (10.32) of AD over ZRB, followed by Sand ( $D$ , 4.56;  $S$ , 8.32), and the lowest is for Clay ( $D$ , 3.24;  $S$ , 5.13). In addition, the distribution of drought characteristics for Sand ( $D$ , 1–9;  $S$ , 2–20) and Loam ( $D$ , 1–11;  $S$ , 2–23) is relatively uniform, whereas Clay tends to concentrate on lower  $D$  of 2–4 months and  $S$  of 1–7, suggesting that Clay shows best performance with higher water holding capacity and drought resistance.

## Discussion

### Comparisons of impacts of land use types on AD

In this study, five different land use types are analyzed (Cropland, Forest, Grassland, Waters, and Urban Land) to evaluate the impacts of AD in semiarid areas. Our findings show that Forest and Grassland are more drought-resistant while Cropland, Waters, and Urban land are more susceptible to severe droughts (Figs. 5, and 6). Adaptation strategies to water deficits and the ability to absorb water can determine drought resistance and recovery capabilities among different vegetation types<sup>52</sup>. In a study published by Hanson and Weltzin et al. (2000), it was shown that vegetation with well-developed roots (e.g., Forest and Grassland) is more resistant to drought and water shortages than vegetation with less-developed roots (e.g., Cropland), which is in accordance with the findings of our study. In addition, Water areas are directly affected by drought resulting in reduced water



**Fig. 8.** Violin graphs of duration and severity of agricultural drought for different soil textures: Sand, Clay, Loam, respectively.

storage, and Urban land may also be more prone to drought due to multiple factors such as high temperature, human activities, precipitation deficit, low humidity, and strong evapotranspiration<sup>53</sup>.

### Comparisons of impacts of soil textures on AD

Our results indicated that Clay performs better than Loam and Sand (Figs. 7, and 8), the reason can be that Clay has good water retention due to smaller pores and low evapotranspiration rate. The finding of Yu et al. (2022) confirmed that Sand has a lower capacity to absorb and store rainfall than the other two soil textures, making it less able to recover from severe AD, while Clay and Loam can recover more quickly due to their better water-holding capacity when replenished by timely precipitation. A number of important implications can be drawn from these results for crop selection and the allocation of soil texture types in the semi-arid region. AD intensity and frequency are closely correlated with soil texture, demonstrating the importance of integrating local soil types, main planting structures, and topographic features into the design of soil moisture monitoring stations so that agricultural management may be improved.

### The impact of other relative factors on AD

Vegetation structure, soil hydrological characteristics and human activities are also the key factors that interact and jointly drive the dynamics of AD. Vegetation regulates water consumption and microclimate through transpiration. The texture and structure of the soil determine the ability of water infiltration, storage and transmission. Human activities directly alter the natural water cycle by changing land use (such as deforestation and urbanization) and water resource management (such as excessive water extraction), often reducing the resilience of ecosystems. The coupling of the three, through positive and negative feedback mechanisms, amplifies or alleviates meteorological drought, jointly determining the occurrence, intensity and recovery process of AD. Therefore, sustainable land management and water resource utilization strategies, such as protecting forests, improving agricultural soil health, and adopting water-saving technologies, are crucial for enhancing the drought resistance of ecosystems.

### Conclusions

In this study, we have analyzed the temporal variations of precipitation, soil moisture, and water shortage in the vadose zone in ZRB on an annual and monthly scale, evaluated the applicability of SWDI in ZRB, and quantitatively assessed the effects of land use type and soil texture on AD. In summary, the following conclusions can be drawn:

- (1) The annual variation trends of soil moisture and precipitation in the ZRB are broadly similar, while the trend for water shortage in the vadose zone is the opposite. Similarly, the interannual distribution of soil moisture and precipitation in the basin is well-consistent. Overall, winter is the most prominent season when soil moisture levels are low in ZRB.
- (2) SWDI is capable of characterizing the water balance of the ZRB soil layer to a certain extent and can be used for AD assessment, monitoring, early warning, and forecasting. To some extent, AD and MD are both beginning and ending at the same time in a specific drought event. However, AD tends to exhibit more severe S than MD.
- (3) Different types of land use in semi-arid areas demonstrate significant impacts of AD. There is a greater drought resistance among Forest and Grassland with lower *D* and *S*, while Cropland, Waters, and Urban

land are more susceptible to severe droughts because of their poorer water holding capacity and human activities.

- (4) Soil texture also has a significant effect on AD. Generally, Sand and Loam are more prone to severe drought with higher *D* and *S* under the similar climate. On the other hand, Clay has better drought resistance toughness.

### Data availability

The data that support the findings of this study are available from the corresponding author (Yimin Hao: 934060679@qq.com) upon reasonable request.

Received: 3 July 2025; Accepted: 27 October 2025

Published online: 26 November 2025

### References

- Crow, W. T., Kumar, S. V. & Bolten, J. D. On the utility of land surface models for agricultural drought monitoring. *Hydrol. Earth Syst. Sci.* **16** (9), 3451–3460. <https://doi.org/10.5194/hess-16-3451-2012> (2012).
- Ezzine, H., Bouziane, A. & Ouazar, D. Seasonal comparisons of meteorological and agricultural drought indices in Morocco using open short time-series data. *Int. J. Appl. Earth Obs Geoinf.* **26**, 36–48. <https://doi.org/10.1016/j.jag.2013.05.005> (2014).
- Willite D.A. Drought as a natural hazard: concepts and definitions. <https://api.semanticscholar.org/CorpusID:8760593> (2000).
- Willite, D. A., Svoboda, M. D. & Hayes, M. J. Understanding the complex impacts of drought: A key to enhancing drought mitigation and preparedness. *Water Resour. Manage.* **21** (5), 763–774. <https://doi.org/10.1007/s11269-006-9076-5> (2007).
- Zhang, J. & Qu, Y. Discussion on the evolution law of drought disaster and the countermeasures of drought relief in China in recent 30 years. *China Flood Drought Manage. (in Chinese)*. **5**, 14. <https://doi.org/10.16867/j.cnki.cfdm.2008.05.014> (2008).
- Guo, Y. et al. Copulas-based bivariate socioeconomic drought dynamic risk assessment in a changing environment. *J. Hydrol.* **575**, 1052–1064. <https://doi.org/10.1016/j.jhydrol.2019.06.010> (2019).
- Hao, L., Zhang, X. & Liu, S. Risk assessment to china's agricultural drought disaster in County unit. *Nat. Hazards.* **61** (2), 785–801. <https://doi.org/10.1007/s11069-011-0066-4> (2012).
- Jiang, W., Wang, L., Feng, L., Zhang, M. & Yao, R. Drought characteristics and its impact on changes in surface vegetation from 1981 to 2015 in the Yangtze river Basin, China. *Int. J. Climatol.* **40** (7), 3380–3397. <https://doi.org/10.1002/joc.6403> (2019).
- Zhao, H. et al. Risk assessment of agricultural drought using the CERES-Wheat model: a case study of Henan Plain, China. *Clim. Res.* **50**, 247–256. <https://doi.org/10.3354/cr01060> (2011).
- Zhou, K., Li, J., Zhang, T. & Kang, A. The use of combined soil moisture data to characterize agricultural drought conditions and the relationship among different drought types in China. *Agric. Water Manage.* **243**, 106479. <https://doi.org/10.1016/j.agwat.2020.106479> (2021).
- Carrão, H., Sepulcre, G., Horion, S. & Barbosa, P. A multitemporal and non-parametric approach for assessing the impacts of drought on vegetation greenness: a case study for Latin America. *EARSeL eProceedings.* **12** (1), 8–24. <https://doi.org/10.12760/01-2013-1-02> (2013).
- Keyantash, J. & Dracup, J. A. The quantification of drought: an evaluation of drought indices. *Bull. Am. Meteorol. Soc.* **83** (8), 1167–1180. <https://doi.org/10.1175/1520-0477-83.8.1167> (2002).
- Sheffield, J., Goteti, G., Wen, F. & Wood, E. F. A simulated soil moisture based drought analysis for the United States. *J. Geophys. Res. Atmos.* **109** (D24), 108. <https://doi.org/10.1029/2004JD005182> (2004).
- Vyas, S. S. et al. A combined deficit index for regional agricultural drought assessment over semi-arid tract of India using geostationary meteorological satellite data. *Int. J. Appl. Earth Obs Geoinf.* **39**, 28–39. <https://doi.org/10.1016/j.jag.2015.02.009> (2015).
- Holzman, M. E., Rivas, R. & Piccolo, M. C. Estimating soil moisture and the relationship with crop yield using surface temperature and vegetation index. *Int. J. Appl. Earth Obs. Geoinf.* **28**, 181–192. <https://doi.org/10.1016/j.jag.2013.12.006> (2014).
- Panu, U. S. & Sharma, T. C. Challenge in drought research: some perspectives and future directions. *Hydrol. Sci. J.* **47**, S19–S30. <https://doi.org/10.1080/02626660209493019> (2002).
- Yan, F., Qin, Z., Li, M. & Wang, Y. Progress in soil moisture Estimation from remote sensing data for agricultural drought monitoring. *J. Nat. Disasters (in Chinese)*. **15** (6). <https://doi.org/10.3969/j.issn.1004-4574.2006.06.020> (2006).
- Yu, M. et al. Agricultural drought of the Poyang lake basin based on large-scale ground monitoring of soil water content. *Adv Water Sci. (in Chinese)*. **33**, 2. <https://doi.org/10.14042/j.cnki.32.1309.2022.02.003> (2022).
- Aghakouchak, A. et al. Remote sensing of drought: progress, challenges and opportunities. *Rev. Geophys.* **53** (2), 452–480. <https://doi.org/10.1002/2014RG000456> (2015).
- Rajsekhar, D., Singh, V. P. & Mishra, A. K. Multivariate drought index: an information theory based approach for integrated drought assessment. *J. Hydrol.* **526**, 164–182. <https://doi.org/10.1016/j.jhydrol.2014.11.031> (2015).
- Shah, R. D. & Mishra, V. Development of an experimental Near-Real-Time drought monitor for India. *J. Hydrometeorol.* **16** (1), 327–345. <https://doi.org/10.1175/JHM-D-14-0041.1> (2015).
- Du, J. et al. Multicomponent satellite assessment of drought severity in the contiguous United States from 2002 to 2017 using AMSR-E and AMSR2. *Water Resour. Res.* **55**, 5394–5412. <https://doi.org/10.1029/2018WR024633> (2019).
- Liu, Y., Liu, Y. & Wang, W. for global drought analysis. *Remote Sens. Environ.* **220**, 1–18. <https://doi.org/10.1016/j.rse.2018.10.026> (2019). Inter-comparison of satellite-retrieved and Global Land Data Assimilation System-simulated soil moisture datasets.
- Luo, L. & Wood, E. F. Monitoring and predicting the 2007 U.S. Drought. *Geophys. Res. Lett.* **34** (22), 1–6. <https://doi.org/10.1029/2007GL031673> (2007).
- Nicolai-Shaw, N., Zscheischler, J., Hirschi, M., Gudmundsson, L. & Seneviratne, S. I. A drought event composite analysis using satellite remote-sensing based soil moisture. *Remote Sens. Environ.* **203**, 216–225. <https://doi.org/10.1016/j.rse.2017.06.014> (2017).
- Yuan, F. et al. Evaluation of hydrological utility of IMERG final run V05 and TMPA 3B42V7 satellite precipitation products in the yellow river source region, China. *J. Hydrol.* **567**, 696–711. <https://doi.org/10.1016/j.jhydrol.2018.06.045> (2018).
- Guo, L. & Lin, H. Chapter two - Addressing two bottlenecks to advance the Understanding of Preferential flow in soils. *Adv. Agron.* **147**, 61–117. <https://doi.org/10.1016/bs.agron.2017.10.002> (2018).
- Li, Q. et al. A 1 Km daily soil moisture dataset over China using in situ measurement and machine learning. *Earth Syst. Sci. Data.* **14** (12), 5267–5286. <https://doi.org/10.5194/essd-14-5267-2022> (2022).
- Ojha, R., Morbidelli, R., Saltalippi, C., Flammini, A. & Govindaraju, R. S. Scaling of surface soil moisture over heterogeneous fields subjected to a single rainfall event. *J. Hydrol.* **516**, 21–36. <https://doi.org/10.1016/j.jhydrol.2014.01.057> (2014).
- Vereecken, H. et al. On the spatio-temporal dynamics of soil moisture at the field scale. *J. Hydrol.* **516**, 76–96. <https://doi.org/10.1016/j.jhydrol.2013.11.061> (2014).
- Martínez-Fernández, J. et al. A soil water based index as a suitable agricultural drought indicator. *J. Hydrol.* **522**, 265–273. <https://doi.org/10.1016/j.jhydrol.2014.12.051> (2015).

32. Baik, J., Zohaib, M., Kim, U., Aadil, M. & Choi, M. Agricultural drought assessment based on multiple soil moisture products. *J. Arid Environ.* **167**, 43–55. <https://doi.org/10.1016/j.jaridenv.2019.04.007> (2019).
33. Li, F., Zhao, Z. M., Jiang, R. & Y. & Influence of irrigation and groundwater on the propagation of meteorological drought to agricultural drought. *Agric. Water Manag.* **277**, 108099. <https://doi.org/10.1016/j.agwat.2022.108099> (2023).
34. Hadadi, F., Moazenzadeh, R. & Mohammadi, B. Estimation of actual evapotranspiration: A novel hybrid method based on remote sensing and artificial intelligence. *J. Hydrol.* **609**, 127774. <https://doi.org/10.1016/j.jhydrol.2022.127774> (2022).
35. Li, Q. et al. A 1 Km daily soil moisture dataset over China using in situ measurement and machine learning. *Earth Syst. Sci. Data.* **14** (12), 5267–5286. <https://doi.org/10.5194/essd-14-5267-2022> (2022).
36. Zhu, Q., Luo, Y., Xu, Y. P., Tian, Y. & Yang, T. Satellite soil moisture for agricultural drought monitoring: assessment of SMAP-derived soil water deficit index in Xiang river Basin, China. *Remote Sens.* **11** (3), 362. <https://doi.org/10.3390/rs11030362> (2019).
37. Durowoju, O. S., Ologunorisa, T. E. & Akinbobola, A. Assessing agricultural and hydrological drought vulnerability in a savanna ecological zone of Sub-Saharan Africa. *Nat. Hazards.* **111**, 2431–2458 (2022).
38. Ying, Z. et al. Developing a conceptual model of groundwater-Surface water interactions in a drought sensitive lowland catchment using multi-proxy data. *J. Hydrol.* **628**, 130550 (2024).
39. Wu, R. & Wu, X. Dynamic prediction of soil moisture under different soil textures in the 463 South of Hehei plain. *Water Resour. Power.* **38** (9), 150–153 (2020).
40. Li, F. & Tao, R. Analysis on factors of hydrological process in Ziya River Basin under changing environment. *Water Res. Protection* (in Chinese), <https://kns.cnki.net/kcms/detail/32.1356.TV.20230302.1605.004.html> (2023).
41. Martínez-Fernández, J., González-Zamora, A., Sánchez, N., Gumuzzio, A. & Herrero-Jiménez, C. M. Satellite soil moisture for agricultural drought monitoring: assessment of the SMOS derived soil water deficit index. *Remote Sens. Environ.* **177**, 277–286. <https://doi.org/10.1016/j.rse.2016.02.064> (2016).
42. Mishra, A., Vu, T., Veettil, A. V. & Entekhabi, D. Drought monitoring with soil moisture active passive (SMAP) measurements. *J. Hydrol.* **552**, 620–632. <https://doi.org/10.1016/j.jhydrol.2017.07.033> (2017).
43. Asadi Zarch, M. A., Sivakumar, B. & Sharma, A. Droughts in a warming climate: a global assessment of standardized precipitation index (SPI) and reconnaissance drought index (RDI). *J. Hydrol.* **526**, 183–195. <https://doi.org/10.1016/j.jhydrol.2014.09.071> (2015).
44. Bloomfield, J. P. & Marchant, B. P. Analysis of groundwater drought Building on the standardised precipitation index approach. *Hydrol. Earth Syst. Sci.* **17** (12), 4769–4787. <https://doi.org/10.5194/hess-17-4769-2013> (2013).
45. Hayes, M. J., Svoboda, M. D., Willite, D. A. & Vanyarkho, O. V. Monitoring the 1996 drought using the standardized precipitation index. *Bull. Am. Meteorol. Soc.* **80** (3), 429–438 (1999). <http://digitalcommons.unl.edu/droughtfacpub/31>
46. Wu, J. et al. Non-linear relationship of hydrological drought responding to meteorological drought and impact of a large reservoir. *J. Hydrol.* **551**, 495–507. <https://doi.org/10.1016/j.jhydrol.2017.06.029> (2017).
47. Li, J. et al. Assessing the responses of hydrological drought to meteorological drought in the Huai river Basin, China. *Theor. Appl. Climatol.* **144**, 1043–1057. <https://doi.org/10.1007/s00704-021-03567-3> (2021).
48. Lloyd-Hughes, B. & Saunders, M. A. A drought climatology for Europe. *Int. J. Climatol.* **22** (13), 1571–1592. <https://doi.org/10.102/joc.846> (2002).
49. Xu, K. et al. Comparative analysis of meteorological and hydrological drought over the Pearl river basin in Southern China. *Hydrol. Res.* **50** (1), 301–318. <https://doi.org/10.2166/nh.2018.178> (2018).
50. Yevjevich, V. M. *An Objective Approach To Definitions and Investigations To Continental Hydrologic Droughts* (Colorado State University, Fort Collins, Colorado, 1967).
51. Chang, J., Li, Y., Wang, Y. & Yuan, M. Copula-based drought risk assessment combined with an integrated index in the Wei river basin, China. *J. Hydrol.* **540**, 824–834. <https://doi.org/10.1016/j.jhydrol.2016.06.064> (2016).
52. Zhang, Q., Kong, D., Singh, V. P. & Shi, P. Response of vegetation to different time-scales drought across china: Spatiotemporal patterns, causes and implications. *Glob Planet. Change.* **152** (5), 1–11. <https://doi.org/10.1016/j.gloplacha.2017.02.008> (2017).
53. Kazemzadeh, M. et al. Detecting drought events over Iran during 1983–2017 using satellite and ground-based precipitation observations. *Atmos. Res.* **269**, 106052. <https://doi.org/10.1016/j.atmosres.2022.106052> (2022).

## Author contributions

**Yuefen Zhang:** Conceptualization, Methodology, Software, Formal analysis, Investigation, Methodology, Writing - Original Draft, Visualization. **Yimin Hao:** Conceptualization, Data Curation, Investigation, Writing - Review & Editing. **Jiyang Tian:** Writing - Review & Editing. **Qingqing Zhang:** Writing - Review & Editing. **Ronghua Liu:** Writing - Review & Editing. **Jianzhu Li:** Writing - Review & Editing.

## Funding

This research was supported by funding from Young Scientists Project of the National Key R&D Program of China (Grant No. 2024YFC3082200) and Open Research Fund Program of Key Laboratory for Water Ecology Management and Protection in River Source Areas, Ministry of Water Resources (Grant No. 2025slbsy06).

## Declarations

## Competing interests

The authors declare no competing interests.

## Additional information

**Correspondence** and requests for materials should be addressed to Y.H. or Q.Z.

**Reprints and permissions information** is available at [www.nature.com/reprints](http://www.nature.com/reprints).

**Publisher's note** Springer Nature remains neutral with regard to jurisdictional claims in published maps and institutional affiliations.

**Open Access** This article is licensed under a Creative Commons Attribution-NonCommercial-NoDerivatives 4.0 International License, which permits any non-commercial use, sharing, distribution and reproduction in any medium or format, as long as you give appropriate credit to the original author(s) and the source, provide a link to the Creative Commons licence, and indicate if you modified the licensed material. You do not have permission under this licence to share adapted material derived from this article or parts of it. The images or other third party material in this article are included in the article's Creative Commons licence, unless indicated otherwise in a credit line to the material. If material is not included in the article's Creative Commons licence and your intended use is not permitted by statutory regulation or exceeds the permitted use, you will need to obtain permission directly from the copyright holder. To view a copy of this licence, visit <http://creativecommons.org/licenses/by-nc-nd/4.0/>.

© The Author(s) 2025